Use of radio occultation for long-term tropopause studies: uncertainties, biases, and instabilities

Paul W. Staten and Thomas Reichler

Department of Meteorology, University of Utah

Corresponding author: Paul W. Staten

Department of Meteorology, University of Utah,

135 S 1460 E, Rm. 819 (WBB), Salt Lake City, UT 84112

e-mail: paul.staten@utah.edu phone: 801-585-1405

January 2007

Submitted to: Journal of Geophysical Research

Special section: Diagnosis and Modeling of the Tropopause: Structure, Dynamics, and Variability

Keywords: radio occultation, tropopause, climate

Abstract

Research suggests that changes in tropopause structure can both indicate and impact changes in the global climate system. The Global Positioning System radio occultation (RO) technique shows tremendous potential for monitoring the global tropopause due to its precision, temporal consistency, and global measurement density. This study examines the capability of RO to monitor the global tropopause by addressing three specific objectives: (1) quantify sources of error in individual RO tropopause measurements, (2) examine absolute bias and long-term stability of RO tropopause parameters with respect to those obtained from radiosondes, and (3) distinguish between errors due to processing and RO instrument differences by comparing tropopause parameters from different RO products. In this study, we make use of data from four different RO missions, including the recent COSMIC (Constellation Observing System for Meteorology, Ionosphere, and Climate). After removing the effects of natural atmospheric variability, the remaining tropopause errors are shown to be related to uncertainties in the RO derived temperature profiles (0.6 K or 150 m) and to the use of a highly nonlinear tropopause definition (1-1.5 K or 300-500 m). Global mean temperature and height biases between RO instruments and radiosondes are within 0.5 K and 75 m. One long-term RO dataset examined in this study has temperature instabilities as large as 2 K, which appear to be due to inconsistent processing. Tropopause measurements from different RO instruments are generally within 30 m and 0.1 K for the globe. Dissimilarly processed temperature data, however, can differ by as much as 2 K in the mean. These results confirm the precision of RO data, but also demonstrate the importance of consistent processing for long-term tropopause temperature studies. Tropopause height data do not appear to be significantly affected by the differences in processing examined in this study.

1. Introduction

Changes in the structure of the tropopause have recently received increased attention both as important factors in climate processes and as sensitive indicators of human induced climate change. For example, changes in the structure of the tropopause may affect stratosphere-troposphere exchange [*Shapiro*, 1980; *Holton et al.*, 1995] and stratospheric moisture content [*Mote et al.*, 1996; *Zhou et al.*, 2001; *Randel et al.*, 2004]. In addition, changes in tropical tropopause height can be linked with variations in strength of the Brewer-Dobson circulation [*Randel et al.*, 2006], increases in the latitudinal extent of the tropical tropopause suggest a widening of the tropical Hadley cell [*Reichler and Held*, 2005; *Seidel et al.*, 2008], and the rising of the tropopause with time has been shown to be a sensitive indicator of human-induced climate change [*Sausen and Santer*, 2003; *Santer et al.*, 2003]. The need for accurate determination of the structure and long-term behavior of the tropopause is clear.

Measuring the global tropopause, however, has been problematic. Radiosondes are often considered the 'gold standard' for measuring tropopause parameters due to their direct, high resolution measurements. However, early radiosondes were often unable to reach the tropopause, and radiosonde products today, while generally of good quality, are expensive and distributed unevenly across the globe. Reanalyses make up somewhat for what radiosondes lack, by providing excellent global spatial and temporal coverage. However, reanalyses are model driven and subject to sudden changes as new data are assimilated [*Sturaro*, 2003; *Sterl*, 2004]. In addition, reanalyses are sometimes of questionable quality [*Trenberth and Caron*, 2001; *Trenberth et al.*, 2001; *Trenberth and Stepaniak*, 2002; *Greatbatch and Rong*, 2006; *Zhao and Li*, 2006], and have low vertical resolution. This low vertical resolution causes reanalyses to miss

important features, such as the recently discovered tropopause inversion layer [*Birner et al.*, 2006].

Global Positioning System radio occultation (RO) is an innovative new technology for monitoring the global atmosphere. RO instruments measure the time delay in occulted signals from one satellite to another. Processing these time delays yields atmospheric bending angle profiles, information which can then be used to derive profiles of atmospheric temperature and moisture, although additional external data is needed to distinguish between the effects of the two. The near absence of moisture in the tropopause region make temperature profiles in that region particularly accurate. In addition, RO data are not susceptible to instrument drift, and do not require instrument calibration [*Anthes et al.*, 2000].

In 1995, the first Earth-observing RO mission, the Global Positioning System Meteorology (GPS/MET) experiment was launched, and until early 1997 produced 100–150 measurements per day (see Figure 1 for a mission timeline). In 2001, the CHAllenging Minisatellite Payload (CHAMP) and the Argentinian Satelitede Aplicaciones Cientificas-C (SAC-C) became operational, and produced roughly 150 and 100 measurements per day, respectively. SAC-C profiles are available through most of 2002, while CHAMP is still operational. In 2006 the Constellation Observing System for Meteorology, Ionosphere and Climate (COSMIC), a constellation of six satellites was launched, and currently produces about 1200 occultations daily across the globe (although it is expected to perform even better in the future, taking as many as 2500 occultations per day).

Ware et al. [1996] and Kursinski et al. [1997] examined profiles from GPS/MET and found RO to be quite accurate (within 1 K) for measuring atmospheric temperatures between 5–15 km. Hajj

et al. [2004] followed up on their work, presenting a detailed characterization of the precision of RO data using CHAMP and SAC-C. They found the accuracy of RO to be within 0.5 K between 5 and 20 km.

Several studies have also been performed, using RO data to study the tropopause region. Randel et al. [2003] used GPS/MET and Schmidt et al. [2004] used CHAMP data to study the mean structure and variability of the tropical tropopause. In addition, Randel et al. [2006] used RO data to document the occurrence, mean height, and mean temperature of multiple tropopauses. However, none of these studies examine the sources and structure of RO tropopause errors.

One such source of error in RO tropopause measurements is data processing. RO temperature data are not direct measurements, but derived from the time delay of a signal. Thus the choice of processing method plays a significant role in the final temperature output. Von Engeln [2006] highlighted this structural uncertainty, and found troubling differences in lower tropospheric and upper stratospheric temperature products processed with different algorithms from the same data.

In the present study, we seek to address the suitability of RO data for the study of long-term tropopause trends by addressing three specific objectives.

- **Objective 1.** Determine the magnitude, structure, and sources of error in individual RO tropopause measurements.
- **Objective 2.** Characterize the absolute error and long-term stability of RO tropopause parameters with respect to those measured by radiosondes.
- **Objective 3.** Distinguish between the contributions of processing and instrument differences to errors between different RO products.

Our paper is organized as follows. In section 2 we describe the data used in our study, and in section 3 we outline our methods. In section 4 we present our results, followed by a discussion of these results in section 5. We summarize and offer our conclusions in section 6.

2. Data

In our study, we make use of moisture-corrected atmospheric temperature profile datasets derived from several RO instruments and provided by the UCAR COSMIC Data Analysis and Archive Center (CDAAC) and by the GFZ Potsdam Information Systems and Data Center (ISDC). These profiles have a 100 m or 200 m vertical resolution, and use atmospheric analyses or forecast models to estimate the relative contributions of moisture and temperature to the measured bending angle. While the difference between the moisture-corrected and the 'dry' profiles is very small in the tropopause region, we use the moisture-corrected profiles in this case to provide the best possible comparison with radiosonde data.

The RO data we use in this study are processed in a variety of different ways, which we group into three categories: near-real-time, post-processed, and ISDC. The near-real-time processing methods change with time and are intended mainly for forecasting purposes. CDAAC provides GPS/MET, SAC-C, CHAMP, and COSMIC data processed near-real-time. In addition, CDAAC also frequently reprocesses their CHAMP and COSMIC datasets with the intent to provide consistent, high quality, post-processed data for use in climate studies. ISDC also reprocesses their data, but not to the same extent as CDAAC. See Table 1 for a list of RO datasets used in this study.

In order to examine the biases of the above RO datasets, we need a reference dataset. For this purpose, we use radiosonde data from the Integrated Global Radiosonde Archive [*Durre et al.*,

2006]. These data (hereafter denoted radiosondes) are characterized by their consistency, as well as their reasonable spatial and temporal coverage.

3. Methodology

To obtain the tropopause parameters for use in this study, we apply the WMO lapse rate tropopause criterion [*WMO*, 1957] to the RO temperature profiles from CDAAC and ISDC, considering only the lowest tropopause in each profile. We use a tropopause detection algorithm based on that used by Reichler et al. [2003], interpolating between vertical levels to determine the pressure and temperature of the tropopause. Radiosonde tropopauses are already reported from high resolution data using the WMO criterion, and we use the reported parameters for our radiosonde tropopauses. For both RO and radiosonde tropopause data, we consider tropopauses above 75 hPa or below 450 hPa as outliers and omit them.

The results for our study are all concerned with differences between nearby tropopause measurements from the above datasets. We thus need to define what classifies measurements as "nearby" for our purposes. Rocken et al. [1997] use a 4° latitude and longitude radius, and ±6 hr time window, while Hajj et al. [2004] compare measurements within 200 km and 30 min of one another. However, neither of these studies focus on the tropopause, and neither had available the high resolution data from COSMIC.

In this study we use a collocation requirement of 150 km and ±6 hr. This requirement is based on the observed variability in the tropopause parameters themselves as measured by COSMIC (see section 4.2.1). Our choice represents a compromise between precision and quantity; tightening the collocation requirements naturally yields smaller errors, but it also reduces the number of nearby measurements and thus the robustness of our statistical analysis. At this stage, we apply

one additional filter to our data; we ignore tropopause matches differing by more than 175 hPa, as these almost certainly are not measurements of the same physical tropopause.

We next bin the differences between measurements for specific regions and seasons, count the number of differences N in each bin, and calculate root mean square (RMS) difference and mean difference μ for each bin. We can derive the standard deviation s for our differences using the identity $s^2 = RMS^2 - \mu^2$, and then compute a two-sided 95% confidence interval width w for the differences from:

$$w = t\sqrt{\frac{s^2}{N}},$$

where t is the t-value from t-statistics, assuming our differences are independent. While this assumption may be called into question, we justify it for the sake of generating useful statistics, and since the actual amount of dependence is difficult to quantify.

4. Results

4.1 A theoretical RO error estimate

To assist us in determining the sources of error in individual tropopause measurements (see Objective 1), we begin by discussing a conceptual tropopause model used by Shepherd [2002]. In this model, the actual temperature profile about a tropopause is approximated above and below by constant lapse rates (see Figure 2), and the tropopause is depicted geometrically as just the vertex of temperature profile line segments in a height-temperature plane. Although a highly simplified view of the tropopause, this is useful for describing the magnitude and cause of changes in tropopause height and temperature [*Gettelman et al.*, 2008]. Here, we use this model

in order to estimate the amount of uncertainty in tropopause height measurements due strictly to RO temperature uncertainties in the tropopause region.

When comparing two model tropopauses in the same plane (see Figure 2), it is evident that a change in tropopause height ΔZ and temperature ΔT depends only on the changes in temperatures ΔT_s above and ΔT_t below the tropopause and on the lapse rates γ_s above and γ_t below the tropopause, where the lapse rate γ is defined as $\gamma = -\frac{\partial T}{\partial Z}$. Specifically, the temperature ΔT can be expressed as $\Delta T_t - \Delta Z \gamma_t$ or as $\Delta T_s - \Delta Z \gamma_s$. Setting these two expressions equal to each other and rearranging yields the following expressions:

$$\Delta Z = \frac{\Delta T_t - \Delta T_s}{\gamma_t - \gamma_s}, \tag{1}$$

and

$$\Delta T = \frac{\Delta T_s \gamma_t - \Delta T_t \gamma_s}{\gamma_t - \gamma_s}.$$

These expressions can be further simplified to analyze the sensitivities of tropopause parameters to perturbations above and below the tropopause [*Austin and Reichler*, 2008], but for our purposes we focus mainly on (1). We first point out that a change in height is maximized by opposing temperature changes above and below the tropopause. If we consider the average tropopause height error δZ to be half the distance between the highest and lowest possible tropopauses given our temperature error δT, then from (1), we have

$$\delta Z = \frac{2\delta T}{|\gamma_t - \gamma_s|}. \tag{2}$$

From Hajj et al. [2004], individual profiles from CHAMP and SAC-C are precise to within 0.6 K between 5 and 20 km, after natural atmospheric uncertainty has been removed. If we let $\delta T =$

$0.6\ \mathrm{K}$, and let $\gamma_t = 6.5\ \mathrm{Kkm^{-1}}$ and $\gamma_s = 0$ in the high latitudes and $\gamma_t = 4\ \mathrm{Kkm^{-1}}$ and $\gamma_s = -4\ \mathrm{Kkm^{-1}}$ in the Tropics, then from (2) we can estimate RO tropopause height errors in high latitudes to be within 180 m and in the Tropics within 150 m.

This estimate utilizes a highly simplified tropopause model, and does not account for errors due to the highly nonlinear, threshold definition of the tropopause (i.e. two very similar temperature profiles can have very different tropopauses) or errors due to the natural variability of the atmosphere in space and time. Our RO errors determined in the following sections will include these additional errors, and by comparing these errors to those described above, we will be able to quantify the different sources of error.

4.2 RO tropopause self-comparisons

In this section, we continue to address Objective 1 by examining measurement differences from individual RO instruments. We focus mainly on data from COSMIC because of its high global measurement density. We will first examine how errors in RO temperature and height vary with distance in space and time. This will allow us to estimate the actual errors in individual tropopause measurements and the effect of natural atmospheric variability. We will then briefly examine the geographical structure of tropopause height and temperature errors.

4.2.1 RO tropopause errors by distance in space and time

To discuss the temporal and spatial structure of RO tropopause errors, we use CHAMP data and focus on the Northern Hemisphere (NH) high latitudes (60°N - 90°N) and on the Tropics (24°S-24°N) during DJF (see Figure 3). We calculate RMS differences in COSMIC tropopause parameters and present the results binned by distance in space and time.

In DJF, the number of matching measurements (Figure 3a, d) increases with distance, but not strictly with separation in time. In the DJF NH high latitudes, the RMS errors in height (Figure 3b) and temperature (Figure 3c) increase with separation in space and time, as one would expect. In the Tropics (Figure 3e, f) the increase in RMS errors with distance is obvious, but the trend with separation in time is not as clear. In the high latitudes, RMS error contours have a fairly well defined slope, indicating that tropopause fluctuations propagate at characteristic phase speeds. We have shown the number of measurements in each bin (Figure 3a, d) In all cases, errors tend to some non-zero value as the separation in space and time approaches zero. Applying a planar fit to this data and extrapolating to zero yield RMS temperature (geopotential height) errors near 1.7 K (480 m) in the NH high latitudes and 1.6 K (510 m) in the Tropics. These values are roughly three times larger than the estimates from using the conceptual tropopause model described in the preceding section. RMS errors in the NH Subtropics (24°N - 60°N, not shown) are even higher (about 2.3 K or 800 m) due to the occurrence of double tropopauses and the resulting strongly discontinuous nature of the first tropopause there [*Schmidt et al.*, 2006; *Randel et al.*, 2007]. Mean biases (not shown) do not show any obvious pattern in space and time.

The planar approximation also gives us a convenient estimate of the slope of the RMS contours in Figure 3, and thus of the characteristic phase speed of tropopause disturbances. Phase speeds for NH disturbances are estimated in this way to be about 8 ms^{-1}, and for the Tropics to be much smaller (2 ms^{-1}) and less well defined. Phase speeds are largest in the NH high latitudes during DJF, consistent with a strengthening of the westerlies.

4.2.2 Geographical RO tropopause error structure

We now analyze the global distribution of collocated tropopause measurements and their RMS errors, using the 150 km and ±6 hr window we described in our methods. Here, we focus on COSMIC data from DJF, with measurements binned in 30° latitude, longitude bins (Figure 4). The number of measurements (Figure 4a) follows a clear meridional pattern, with the most measurements in the Subtropics and the least in the Tropics. The RMS errors in tropopause height (Figure 4b) are generally on the order of 500 m, and RMS errors in tropopause temperature (Figure 4c) range from 1 K to greater than 2.5 K, with the bulk around 1.5 K. Height and temperature errors also show a meridional structure, with higher values in the Subtropics. Again, these higher RMS errors in the Subtropics are likely related to the occurrence of double tropopauses.

4.3 Meridional error structure of RO when compared to radiosondes

In order to understand the absolute error of different RO datasets (see Objective 2), we now examine the meridional error structure in RO-derived tropopause heights and temperatures by comparing the different RO products to radiosonde measurements. We examine the zonal, seasonal, 3° latitude mean temperature and height biases between RO and radiosonde tropopauses, as well as the 95% confidence intervals for those mean biases. We also examine the RMS errors between RO and radiosonde tropopause parameters by latitude and season. The seasonal data is calculated from all instances of each season during the time span of each RO product. When displaying our zonal mean biases, RMS differences, and confidence intervals, we apply a 30° latitude wide Gaussian smoothing.

We begin our comparison by considering the tropopause height and temperature biases between the four RO instruments from CDAAC – GPS/MET, SAC-C, CHAMP, and COSMIC – and

radiosondes (see Figure 5). Biases in CHAMP and COSMIC tropopause height are generally quite small; COSMIC tropopause height biases are the only biases never larger than 200 m in the global mean, COSMIC height biases are also slightly negative (ca. –75 m). Confidence interval widths for the mean height biases have decreased strongly since GPS/MET; GPS/MET confidence intervals are generally quite large (from 200 m to more than 1 km), and at times undefined (as in the far Southern latitudes) due to the lack of data. On the other hand, confidence interval widths for COSMIC mean height biases are quite small (as small as 20 m).

Temperature biases between the same four RO instruments and radiosondes (Figure 6) show a much more distinct meridional structure. Zonal mean temperature biases between both GPS/MET and CHAMP and radiosondes tend to be cool in the high latitudes (nearly –2 K at the poles) and are often warm everywhere else (by as much as 3 K, or 4 K in the case of GPS/MET). CHAMP and COSMIC show generally warm biases (0.5 and 0.25 K, respectively) when compared to radiosondes, although CHAMP and COSMIC biases are never larger than 1.5 K and 1 K, respectively. Confidence intervals for the mean temperature biases show an improvement with products in time similar to those for height described above, with the confidence interval width for COSMIC mean temperature biases against radiosondes reaching values as small as 0.6 K in the NH Extratropics.

To determine the factors that determine the biases and confidence intervals shown above, we now investigate the meridional distribution of the collocated RO and radiosonde measurements used above, as well as the meridional structure of RMS errors in height and temperature. The meridional measurement distribution (Figure 7) clearly reflects the high density of radiosonde stations over land surfaces in the NH. The thickness of the GPS/MET vs. radiosonde and SAC-C vs. radiosonde confidence intervals over the Southern Hemisphere and the narrowness in the NH

are due to the much smaller and larger numbers of measurements at those latitudes. However, in the NH Subtropics, measurement density is reasonably high, so the noticeable width of the height and temperature confidence intervals must be due to increased errors at those latitudes.

This is confirmed upon examination of the RMS errors in tropopause height and temperature of the different RO products with respect to radiosondes (Figure 8, 9). The Subtropics are regions of consistently high RMS errors between RO datasets and radiosondes. We point out that in general, the RMS errors for the different comparisons are fairly similar; they are not orders of magnitude different, as some of the confidence interval widths in Figures 5 and 6 are. However, we do note that CHAMP and COSMIC RMS temperature and height errors do not vary much from season to season, while GPS/MET and SAC-C RMS height and temperature errors demonstrate large seasonal differences.

4.4 Meridional error structure between RO products

Now that we have examined the absolute biases for RO instruments using radiosonde data, we compare tropopause height and temperature data between different RO instruments in order to quantify the errors between instruments as part of Objective 3. Although we consider four RO instruments in this study, only two sets of instruments have any temporal overlap: CHAMP and SAC-C, and CHAMP and COSMIC. Here we do not examine seasonal biases, since the comparisons take place over mostly different seasons and the number of measurements for the SAC-C and CHAMP intercomparison is quite small. Rather, we show the mean biases based on the entire time period in which the two products overlap. We compare tropopause height and temperature biases of SAC-C and of COSMIC, using CHAMP as a reference (Figure 10). Height biases (Figure 10a) between SAC-C and CHAMP are just as small as those between COSMIC

and CHAMP (~30 m). Temperature biases (Figure 10b) between CHAMP and SAC-C show a considerably different pattern, with cold biases (–2 K) in the high latitudes and warm biases (2-4 K) in the Tropics, resembling the bias patterns of both GPS/MET and SAC-C against radiosondes (Figure 6).

It should be noted that SAC-C is processed in near-real-time, while CHAMP and COSMIC data are both post-processed; thus the larger temperature biases between SAC-C and CHAMP are somewhat expected. To estimate how much of the differences can be ascribed to different processing methods, we examine the height and temperature biases between near-real-time COSMIC and post-processed COSMIC data (Figure 11), with the post-processed data as our reference. We do not show confidence intervals for these biases, but do note that their widths are all within ±0.2 K due to the high density of COSMIC measurements. Biases in tropopause height in the near-real-time data (solid lines) are generally small (+20 m), except in the high latitudes during SON. Biases in near-real-time temperature (dashed lines) for MAM (SON) are about 0.1 K (1 K) for the Tropics and –0.4 K (–2 K) for high latitudes. Similar temperature biases are evident in the temperature comparison between SAC-C and CHAMP (Figure 10b), GPS/MET and radiosondes (Figure 6), and SAC-C and radiosondes (Figure 6), suggesting that most of the actual temperature biases between different RO instruments result from processing differences.

4.5 Long-term CHAMP temperature stability

Now that we have shown the effect of processing on RO errors, we are ready to address the instrument stability concern in Objective 2. Here, we examine the mean tropopause temperature bias between CHAMP – our only long-term RO dataset – and radiosondes by latitude and season (Figure 12). Temperature biases between post-processed CHAMP and radiosondes (Figure 12a)

show strong shifts. In particular, we note the abrupt shifts in JJA 2005 and MAM 2006, where biases change by as much as 3 K. Height biases (not shown) show no such sudden change; i.e. they appear to be much more stable in time.

The intent of post-processed RO datasets is to provide as stable and accurate a dataset as practically possible for climate studies. Therefore, the processing methods used should kept constant over the entire analysis period, as is done for reanalysis data. The existence of dramatic bias shifts in the CHAMP data, however, would be most easily explained by changes in processing methods. To investigate whether this is indeed the case, we compare the temperature data from CHAMP processed by the ISDC with temperatures from radiosondes (Figure 12 b). The bias pattern in the ISDC CHAMP data is qualitatively and quantitatively similar to the bias pattern present in the near-real-time CDAAC data, suggesting some similarity in processing. Although the data from ISDC are somewhat more variable in time than the post-processed data, they do not exhibit unusual shifts in time. This suggests that the instability shown in the post-processed data is not due to instrumentation or our methods, but due to processing.

4.6 Quality of radiosonde data

Digressing from our main objectives for a moment, we point out one additional result from our study. In addition to their use for examining RO tropopause data, our methods are also useful for examining the regional error structure of tropopause parameters as measured by radiosondes. To do this, we use COSMIC as our reference and examine the regional pattern of mean biases between radiosondes and COSMIC. We show here only results for DJF 2006 (Figure 13) since the other seasons are qualitatively very similar. While height biases for the individual regions are generally of the same order as those for the zonal mean biases (Figure 5), India's radiosonde

network exhibits exceptionally strong and consistently negative biases; several between –1 km and –2 km. Temperature biases (not shown) are consistently too warm over much of India (about +4 to +7 K) as well. Our results substantiate those mentioned in Kuo et al. [2005] and support using RO data to characterize differences between radiosonde products.

5. Discussion

In this section, we discuss the results shown in our previous section, and how they address each of our objectives.

5.1 Magnitude, structure, and sources of error in RO tropopause measurements

In section 4.1, we use a conceptual tropopause model to estimate the errors in RO tropopause height precision to be about 150–180 m, based on an RO temperature precision of 0.6 K [*Hajj et al.*, 2004]. In section 4.2.1, we examine matching COSMIC data, and determine that the actual errors in determining tropopause temperature (height) for the same location and time are closer to 1.7 K (480 m) in the NH high latitudes and 1.6 K (510 m) in the Tropics. Previous studies found tropopause parameter errors between RO and radiosondes to be in the neighborhood of 2–4 K [*Randel et al.*, 2003; *Schmidt et al.*, 2005] and 700 m, and tropopause temperature errors in radiosonde data to be roughly the same, at ~2–3 K [*Tsuda et al.*, 1994].

We explain this wide range in values with three sources of uncertainty: Instrument error, tropopause definition uncertainty, and natural atmospheric variability. By instrument error, we mean the uncertainty in RO temperature measurements in the vicinity of the tropopause, and the resulting uncertainty in height based on the conceptual tropopause model in section 4.1. Tropopause definition uncertainty arises from the sensitive, nonlinear definition of the tropopause involving a fixed threshold; an instrument can record two arbitrarily similar

temperature profiles and still record very different tropopauses. Natural atmospheric variability is simply related to the naturally occurring variability of the atmosphere in space and time and the resulting differences between two "nearby" measurements.

The 0.6 K figure from Hajj et al. [2004] and the corresponding height errors of 150-180 m are achieved by filtering out natural variability, and are thus estimates of instrument errors only. On the other hand, the 1.6 K figure obtained in this study is an estimate of the actual uncertainty in RO tropopause measurements at the same place and time, and thus includes instrument errors and tropopause definition uncertainty. The larger (~3 K) errors reported by Randel et al. [2003] and Schmidt et al. [2005] also include errors due to natural atmospheric variability, which will vary depending on the collocation requirement used. By considering the different error sources discussed above and by accepting an instrument temperature (height) error of 0.6 K (150 m) [*Haji et al.*, 2004], we estimate the errors due to tropopause definition uncertainty to be 1–1.5 K (300–500 m). For our 150 km and ±6 hr collocation requirement, we can estimate (from Figures 3 and 4) that natural uncertainty adds an additional 0.5–1 K (300–400m). However, we caution that these are global mean estimates, and that actual uncertainties vary strongly with latitude. See Table 2 for a summary of the different sources of error and their respective magnitudes.

We now address how future tropopause climate studies may reduce these sources of error. Unfortunately, as long as a one uses a temperature-based tropopause definition, or is interested in RO-derived tropopause temperatures, instrument temperature errors will remain. However, Narayana Rao et al. [2007] construct a bending angle tropopause definition, which may be useful for studying long-term tropopause height trends, as the RO bending angle is not subject to the same degree of error as the RO derived temperature. Errors stemming from tropopause definition uncertainty may be reduced by adding additional filters to the data, i.e., examining strictly the

Tropical or an Extratropical tropopause, or by defining a tropopause "strength" threshold, to avoid tropopauses that are likely to be missed in nearby observations. Calculating a "climatological tropopause" from time-mean temperature profiles would also likely reduce much of the error due to tropopause uncertainty; time-averaging eliminates the fine structure responsible for the tropopause uncertainty we defined here. Natural uncertainty must always be considered, but may be reduced through high sampling density and strict collocation criteria.

5.2 Absolute error and long-term stability of RO tropopause parameters

In order to put the following discussion in perspective, we first mention that the temperature stability requirement for climate studies in the troposphere is 0.04 K according to Ohring et al. [2005]. In other words, if the bias in a dataset changes by more than 0.04 K per decade, it is probably unsuitable for climate studies. However, this stability requirement is related to measurement of surface temperature changes associated with global climate change, and we relax the requirement here, as tropopause temperature trends are stronger; –0.5 K per decade at the tropopause [*Seidel and Randel*, 2006] as opposed to +0.13 K per decade at the surface [*Solomon et al.*, 2007]. Accordingly, we consider any change in tropopause temperature biases larger than 0.2 K to be seriously detrimental for use in climate studies. Using our conceptual tropopause model, we estimate a 0.2 K bias shift to be equivalent to a height shift of about 60 m.

We now proceed to discuss the absolute errors of RO tropopause parameters based on our comparison with radiosonde data. Global mean height biases between COSMIC and radiosondes are fairly small, and slightly negative (–75 m). Temperature biases of GPS/MET and SAC-C against radiosondes are relatively large due to processing, while those for CHAMP and COSMIC are generally smaller and somewhat warm (0.25 K for COSMIC, 0.5 K for CHAMP). Similar

biases (–100 m and 0.6 K) were noted for RO derived cold point tropopause parameters in Randel et al., [2003]. These absolute errors in RO height and temperature are in all cases larger than the stability requirements we specified above, and we cannot discount these errors when considering tropopause data from RO and radiosonde datasets.

While mean biases in post-processed datasets appear small, we show in Section 4.5 that tropopause temperature biases between post-processed CHAMP and radiosondes show sudden shifts as large as ±2.5 K. Thus, post-processed CHAMP temperatures do not meet our temperature stability requirements for tropopause research. On the other hand, tropopause temperature biases between ISDC CHAMP and radiosondes do not exhibit a clear trend during 2001–2007. Similarly, height biases in both CHAMP datasets exhibit no trends.

5.3 Sources of uncertainty between RO products

Finally, we discuss the errors in tropopause parameters measured by different RO instruments. The two instrument comparisons we have available illustrate the effects of comparing similarly and dissimilarly processed datasets. In both cases height biases are quite small; global average biases between RO products are about 30 m. Biases in temperature between dissimilarly processed datasets can be as large as 2.5 K, while for similarly processed datasets they are on the order of 0.1 K, as in Hajj et al. [2004]. Thus, height biases between RO tropopause datasets, whether processed similarly or not, meet the stability requirement we specified above. Temperature biases for similarly processed datasets are also within the required limits, while temperature biases for dissimilarly processed datasets are well outside the required range.

6. Summary and conclusion

In our introduction we state the three primary objectives of our study: (1) determine the magnitude, structure, and sources of error in RO tropopause measurements, (2) characterize the absolute error and long-term stability of RO tropopause parameters with respect to those measured by radiosondes, and (3) distinguish between the contributions of processing and instrument differences to errors between different RO products. We now summarize our results for each objective, and conclude with suggestions for future tropopause climate studies.

Objective 1: We find that uncertainties in tropopause parameter measurements are due mostly to the nonlinearity of the tropopause definition (ca. 48%) and to natural variability in the atmosphere (ca. 28%), although instrument uncertainties (ca. 24%) do add a significant error component as well.

Objective 2: We examine the time-mean meridional error structure in RO height and temperature against radiosonde, and find generally good agreement in tropopause, aside from noise, and a negative (70 m) bias in tropopause height in RO data. We see that RO processing methods strongly affect temperature biases between RO and radiosonde data, with near-real-time data having large warm (cool) bias in the Tropics (Extratropics). Post-processed data exhibit warm biases of 0.25–0.5 K against radiosondes. These biases agree well with those determined by Randel et al. [2003].

Upon examining the temporal structure of zonal mean tropopause parameter biases between post-processed CHAMP data and radiosondes, we find no noticeable instability in height biases, but very strong instabilities in temperature biases (2.5 K), which appear to be due to errors or inconsistencies in processing. ISDC CHAMP tropopause temperatures, when compared to those

from radiosondes, show no such instabilities. If these bias instabilities are real, one should be cautious when utilizing the CDAAC post-processed CHAMP data for tropopause climate studies.

Objective 3: We find that tropopause heights in different RO instruments are sufficiently similar (within ~30 m) for the straightforward combination of RO datasets for use in tropopause height studies without regard to the processing methods used. RO tropopause temperature datasets, on the other hand, are only similar enough to be combined for long-term studies if the products are processed similarly.

Future studies may reduce uncertainty in measured tropopause parameters by filtering data as described in section 5.1, and by considering tropopause heights computed from time-mean temperature profiles, rather than time averages of tropopause heights. It appears that RO tropopause height datasets can freely be combined regardless of their respective levels of processing. To study RO tropopause temperature trends, however, one must combine similarly processed datasets. Since the current post-processed CHAMP dataset does not appear stable enough for tropopause climate studies, we propose considering the combination of near-real-time and ISDC processed RO tropopause temperature data. Fortunately, CDAAC reprocesses their datasets frequently, and the instability in post-processed CHAMP data are likely to be eliminated in the near future.

Acknowledgments

The author would like to thank NCAR, GFZ Potsdam, and NOAA for use of their RO data, and Doug Hunt and the CDAAC team for their discussion of CHAMP data. We also thank Chuntao Liu for his assistance, and Dian Seidel and John Horel for their helpful comments. This work

was supported by NASA Headquarters under NASA Earth and Space Science Fellowship Program – Grant 07-Earth07F-0108 and by NSF Grant ATM 0532280.

References

Anthes, R.A., C. Rocken, and Y.H. Kuo (2000), Applications of COSMIC to Meteorology and Climate, *Terrestrial, Atmospheric and Oceanic Sciences*, *11*, 115-156.

Austin, J. and T. Reichler (2008), Simulations of long-term variability in the cold point tropical tropopause, *J. Geophys. Res.*, submitted.

Birner, T., D. Sankey, and T. G. Shepherd (2006), The tropopause inversion layer in models and analyses, *Geophys. Res. Lett.*, *33*, L14804, doi:10.1029/2006GL026549.

Durre I., R. S. Vose, and D. B. Wuertz (2006), Overview of the Integrated Global Radiosonde Archive, *J. Climate*, *19*, 53-68.

Hajj, G. A., C. O. Ao, B. A. Iijima, D. Kuang, E. R. Kursinski, A. J. Mannucci, T.K. Meehan, L. J. Romans, M. de la Torre Juarez, T. P. Yunck (2004), CHAMP and SAC–C atmospheric occultation results and intercomparisons, *J. Geophys. Res.*, *109*, D06109, doi:10.1029/2003JD003909.

Gettelman, A., et al. (2008), The tropical tropopause layer 1960-2100, *Atmos. Chem Phys. Discuss.*, submitted.

Greatbatch, R. J., and P.P. Rong (2006), Discrepancies between different Northern Hemisphere summer atmospheric data products, *J. Climate*, *19*(7), 1261

Holton, J.R., P. H. Haynes, M. E. McIntyre, A. R. Douglass, R. B. Rood, L. Pfister (1995), Stratosphere-troposphere exchange, *Rev. Geophys.*, *33*, 403-439.

Kuo, Y. H., W. S. Schreiner, J. Wang, D. L. Rossiter, and Y. Zhang (2005), Comparison of GPS radio occultation soundings with radiosondes, *Geophys. Res. Lett.*, *32*, L05817

Kursinski, E. R., G.A. Hajj, J.T. Schofield, R.P. Linfield, K.R. Hardy (1997), Observing Earth's atmosphere with radio occultation measurements using the Global Positioning System, *J. Geophys. Res.*, *102*(D19), 23429-23465

Mote, P. W., K. H. Rosenlof, J. R. Holton, R. S. Harwood, and J. W. Waters (1996), An atmospheric tape recorder: The imprint of tropical tropopause temperatures on stratospheric water vapor, *J. Geophys. Res.*, *101*, 3989–4006.

Narayana Rao, D., M. V. Ratnam, B. V. K. Murthy, V. V. M. J. Rao, S. K. Mehta, D. Nath, and S. G. Basha (2007), Identification of tropopause using bending angle profile from GPS radio occultation (RO): A radio tropopause, *Geophys. Res. Lett.*, *34*, L15809, doi:10.1029/2007GL029709.

Ohring, G., B. Wielicki, R. Spencer, B. Emery, and R. Datla (2005), Satellite instrument calibration for measuring global climate change, *Bull. Am. Meteorol. Soc.*, *86(9)*, doi:10.1175/BAMS-86-9-1303.

Randel, W. J., D. J. Seidel, L. L. Pan (2007), Observational characteristics of double tropopauses, *J. Geophys. Res.*, *112*, D07309, doi:10.1029/2006JD007904

Randel, W. J., F. Wu, H. Vömel, G. E. Nedoluha, and P. Forster (2006), Decreases in stratospheric water vapor after 2001: Links to changes in the tropical tropopause and the Brewer-Dobson circulation, *J. Geophys. Res.*, *111*, D12312, doi:10.1029/2005JD006744.

Randel, W. J., F. Wu, S. J. Oltmans, K. Rosenlof, and G. Nedoluha (2004), Interannual changes of stratospheric water vapor and correlations with tropical tropopause temperatures, *J. Atmos. Sci.*, *61*, 2133–2148.

Randel, W. J., F. Wu, W. R. Ríos (2003), Thermal variability of the tropical tropopause region derived from GPS/MET observations, *J. Geophys. Res., 108*, 4024, doi:10.1029/2002JD002595.

Reichler, T., and I. Held (2005), Widening trend of the Hadley cell during the past 40 years. Proc. 17th Conference on Climate Variability and Change, Amer. Meteor. Soc., Cambridge, MA, 16 June.

Reichler, T., M. Dameris, and R. Sausen (2003), Determining the tropopause height from gridded data, *Geophys. Res. Lett., 30*(20), 2042, doi:10.1029/2003GLGL018240.

Rocken, C., et al. (1997), Analysis and validation of GPS/MET data in the neutral atmosphere, *J. Geophys. Res.*, *102*, 29,849-29,866.

Santer, B. D., et al. (2003), Contributions of anthropogenic and natural forcing to recent tropopause height changes, *Science*, *301*, 479-483.

Sausen, R., and B. D. Santer (2003), Use of changes in tropopause height to detect human influences on climate, *Meteorol. Zeitschrift, 12*, 131-136.

Schmidt, T., G. Beyerle, S. Heise, J. Wickert, and M. Rothacher, (2006) A climatology of multiple tropopauses derived from GPS radio occultations with CHAMP and SAC-C, *Geophys. Res. Lett.*, *33*, L04808, doi: 10.1029/2005GL024600

Schmidt, T., J. Wickert, G. Beyerle, and C. Reigber (2004), Tropical tropopause parameters derived from GPS radio occultation measurements with CHAMP, *J. Geophys. Res.*, *109*, D13105, doi:10.1029/2004JD004566.

Schreiner, W., C. Rocken, S. Sokolovskiy, S. Syndergaard and D. Hunt (2007), Estimates of the precision of GPS radio occultations from the COSMIC/FORMOSAT-3 mission, *Geophys. Res. Lett.*, *34*, L04808, doi:10.1029/2006GL027557.

Seidel, D., Q. Fu, W. Randel, and T. Reichler (2008), Widening of the Tropical Belt in a Changing Climate, *Nature Geosci.*, *1*, 21-24.

Seidel, D.J., and W.J. Randel (2006), Variability and trends in the global tropopause estimated from radiosonde data. *J. Geophys. Res.*, *111*, D21101, doi:10.1029/2006JD007363.

Shapiro, M. (1980), Turbulent Mixing within Tropopause Folds as a Mechanism for the Exchange of Chemical Constituents between the Stratosphere and Troposphere, *J. Atmos. Sci.*, *37*, 994–1004.

Shepherd, T. G. (2002), Issues in stratosphere-troposphere coupling, *J. Meteor. Soc. Japan*, *80*, *4B*, 769 – 792.

Solomon, S., et al. (2007), *Climate change 2007: the physical science basis. Contribution of working group I to the fourth assessment report of the Intergovernmental Panel on Climate Change*, Cambridge University Press, Cambridge, UK

Sterl, A. (2004), On the (in-)homogeneity of reanalysis products, *J. Climate*, *17*, 3866–3873.

Sturaro G. (2003), A closer look at the climatological discontinuities present in the NCEP/NCAR reanalysis temperature due to the introduction of satellite data, *Climate Dyn.*, *21*, doi:10.1007/ s00382-003-0348-y.

Trenberth, K. E., and D. P. Stepaniak (2002), A pathological problem with NCEP reanalyses in the stratosphere, *J. Climate, 15*, 690-695.

Trenberth, K. E., D. P. Stepaniak, J. W. Hurrell, and M Fiorino (2001), Quality of reanalysis in the Tropics, *J. Climate, 14*, 1499–1510.

Trenberth, K., E., and J. M.Caron (2001), Estimates of meridional atmosphere and ocean heat transports, *J. Climate, 14*, 3433–43.

Tsuda, T., Y. Murayama, T. Nakamura, R. A. Vincent, A.H. Manson, C. E. Meek, R. L. Wilson (1994), Variations of gravity wave characteristics with height, season and latitude revealed by comparative observations. *J. Atmos. Sol. Terr. Phys.*, *56*, 555-568.

von Engeln, A. (2006), A first test of climate monitoring with radio occultation instruments: Comparing two processing centers, *Geophys. Res. Lett.*, *33*, L22705, doi:10.1029/2006GL027767.

Ware, R., et al. (1996), GPS Sounding of the atmosphere from low Earth orbit: Preliminary results, Bull. *Am. Meteorol. Soc.*, 77, 19-40.

WMO (1957), Meteorology - A three dimensional science, *WMO Bull.*, *6*, 134-138, Geneva, Switzerland.

Zhao, Y., and J. Li (2006), Discrepancy of mass transport between the Northern and Southern Hemispheres among the ERA-40, NCEP/NCAR, NCEP-DOE AMIP-2, and JRA-25 reanalysis, *Geophys. Res. Lett.*, 33, L20804, doi:10.1029/2006GL027287.

Zhou, X. L., M. A. Geller, and M. Zhang (2001), Cooling trend of the tropical cold point tropopause temperatures and its implications, *J. Geophys. Res.*, *106*, 1511–1522.

Captions

Table 1. RO data products used in this study, along the general processing category (see text), starting and ending dates and the number of seasons covered. RT denotes near-real-time data, PP denotes post-processed data, and ISDC denotes data processed at the GFZ Potsdam Information Systems and Data Center.

Table 2. Sources of error in RO tropopause measurements, along with their approximate magnitudes. Also listed are the studies from which these estimates come.

Figure 1. Timeline of different products considered in this study. Arrows indicate that the dataset continues beyond the time shown.

Figure 2. Conceptual tropopause model after Shephard [2002]. The blue lines represent a temperature profile in the viscinity of the tropopause, and the red solid lines represent the profile after hypothetical temperature changes of ΔT_s above and ΔT_t below the tropopause. The black lines represent the resulting changes ΔZ and ΔT in tropopause height and pressure, respectively. The gray lines relate ΔT to ΔT_s, ΔT_t, γ_s, and γ_t as described in the text. The dashed lines are for clarity.

Figure 3. Error statistics for collocated DJF COSMIC tropopause data binned by distance in space and separation in time. The number of measurements are shown in (a) and (d), RMS height errors are shown in (b) and (e), and RMS temperature errors in (f). (a) through (c) are for Northern Hemisphere high latitudes, while (d) through (f) are for the Tropics.

Figure 4. Geographical distribution of measurements and RMS errors for collocated DJF COSMIC tropopause data. Shown are the number of measurements in each bin (a), RMS height errors (b), and RMS temperature errors (c).

Figure 5. Zonal mean geopotential height differences between RO and radiosonde datasets, and the 95% confidence interval for the mean. Profiles are shown for DJF (a), MAM (b), JJA (c), and SON (d). All values are Gaussian smoothed over 30° latitude.

Figure 6. Zonal mean temperature differences between RO and radiosonde datasets, and the 95% confidence interval for the mean. Profiles are shown for DJF (a), MAM (b), JJA (c), and SON (d). All values are Gaussian smoothed over 30° latitude.

Figure 7. Meridional distribution of the average number of matching RO vs. radiosonde measurements per season for each RO instrument during the course of our study.

Figure 8. Meridional profile of RMS height differences between RO and radiosonde data. Profiles are shown for DJF (a), MAM (b), JJA (c), and SON (d). All values are Gaussian smoothed over 30° latitude.

Figure 9. Meridional profile of RMS temperature differences between RO and radiosonde data. Profiles are shown for DJF (a), MAM (b), JJA (c), and SON (d). All values are Gaussian smoothed over 30° latitude.

Figure 10. Zonal mean geopotential height differences (a) and temperature differences (b) between the RO datasets specified for SON. All values are Gaussian smoothed over 30° latitude.

Figure 11. Zonal mean temperature differences between post-processed (PP) and near-real-time (RT) COSMIC data for the seasons shown. Solid lines and left axes show mean height

differences, while dashed lines and right axes show mean temperature differences. All values are Gaussian smoothed over 30° latitude.

Figure 12. Zonal mean tropopause temperature bias between CHAMP and radiosonde data as a function of time and for two different processing methods. Shown are CHAMP biases from CDAAC (a) and ISDC (b).

Figure13. Geographical distribution of mean tropopause height biases between radiosonde and COSMIC data during the period Dec. 2006 – Feb. 2007. Gray cells represent insufficient data.

Tables

Product	Processing	Start	End	Seasons
GPS/MET	RT	1995.152	1996.335	6
SACC	RT	2001.244	2002.244	4
CHAMP	RT	2006.244	2007.150	3
CHAMP	PP	2001.152	2006.334	22
CHAMP	ISDC	2001.152	2006.334	22
COSMIC	RT	2006.244	2007.149	3
COSMIC	PP	2006.244	2007.151	3

625 **Table 1.** RO data products used in this study, along the general processing category (see text), starting and ending dates and the number of seasons covered. RT denotes near-real-time data, PP denotes post-processed data, and ISDC denotes data processed at the GFZ Potsdam Information Systems and Data Center.

Error	ΔT [K]	ΔZ [m]	Source
RO Instrument	0.6	150	Hajj et al., 2004
Tropopause definition	1-1.5	300-500	This study
Natural Variability	0.5 - 1	300-400	This study
Total	2.1-3.1	750-1050	

630

Table 2. Sources of error in RO tropopause measurements, along with their approximate magnitudes. Also listed are the studies from which these estimates come.

Figures

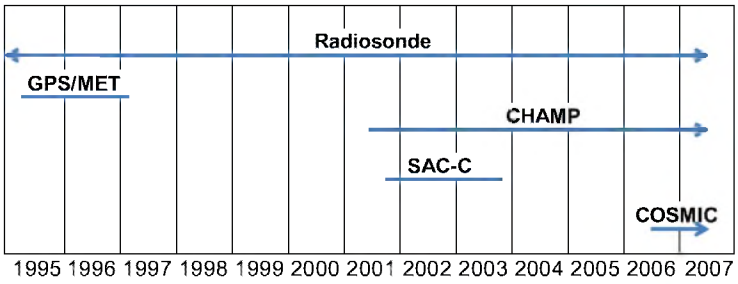

Figure 1. Timeline of different products considered in this study. Arrows indicate that the dataset continues beyond the time shown.

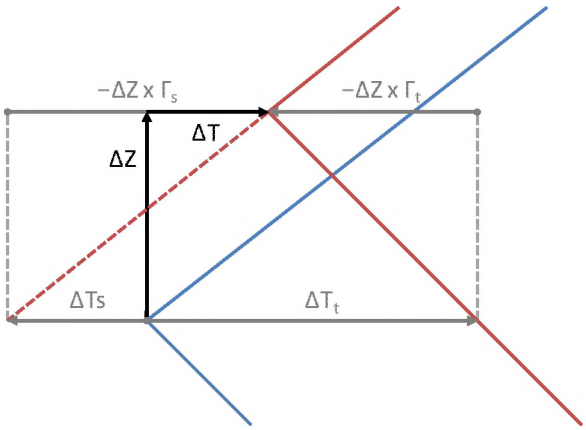

640

Figure 2. Conceptual tropopause model after Shephard [2002]. The blue lines represent a temperature profile in the viscinity of the tropopause, and the red solid lines represent the profile after hypothetical temperature changes of ΔT_s above and ΔT_t below the tropopause. The black lines represent the resulting changes ΔZ and ΔT in tropopause height and pressure, respectively. The gray lines relate ΔT to ΔT_s, ΔT_t, γ_s, and γ_t as described in the text. The dashed lines are for clarity.

645

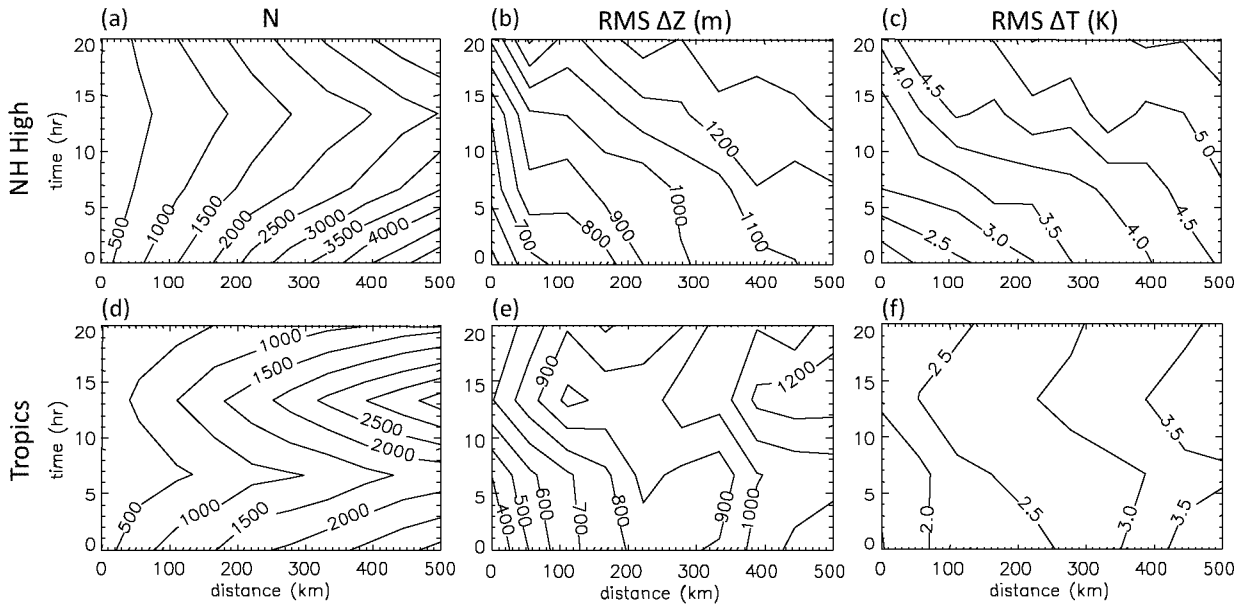

650 **Figure 3.** Error statistics for collocated DJF COSMIC tropopause data binned by distance in space and separation in time. The number of measurements are shown in (a) and (d), RMS height errors are shown in (b) and (e), and RMS temperature errors in (f). (a) through (c) are for Northern Hemisphere high latitudes, while (d) through (f) are for the Tropics.

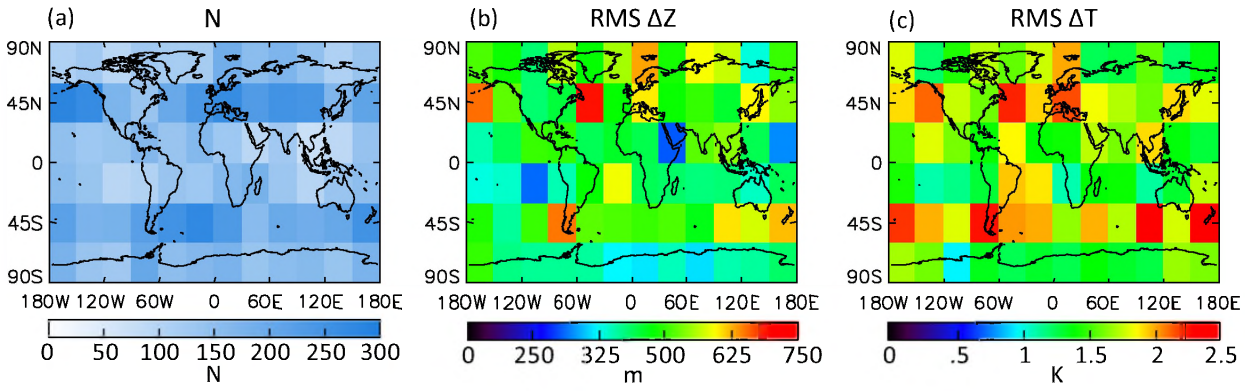

655 **Figure 4.** Geographical distribution of measurements and RMS errors for collocated DJF COSMIC tropopause data. Shown are the number of measurements in each bin (a), RMS height errors (b), and RMS temperature errors (c).

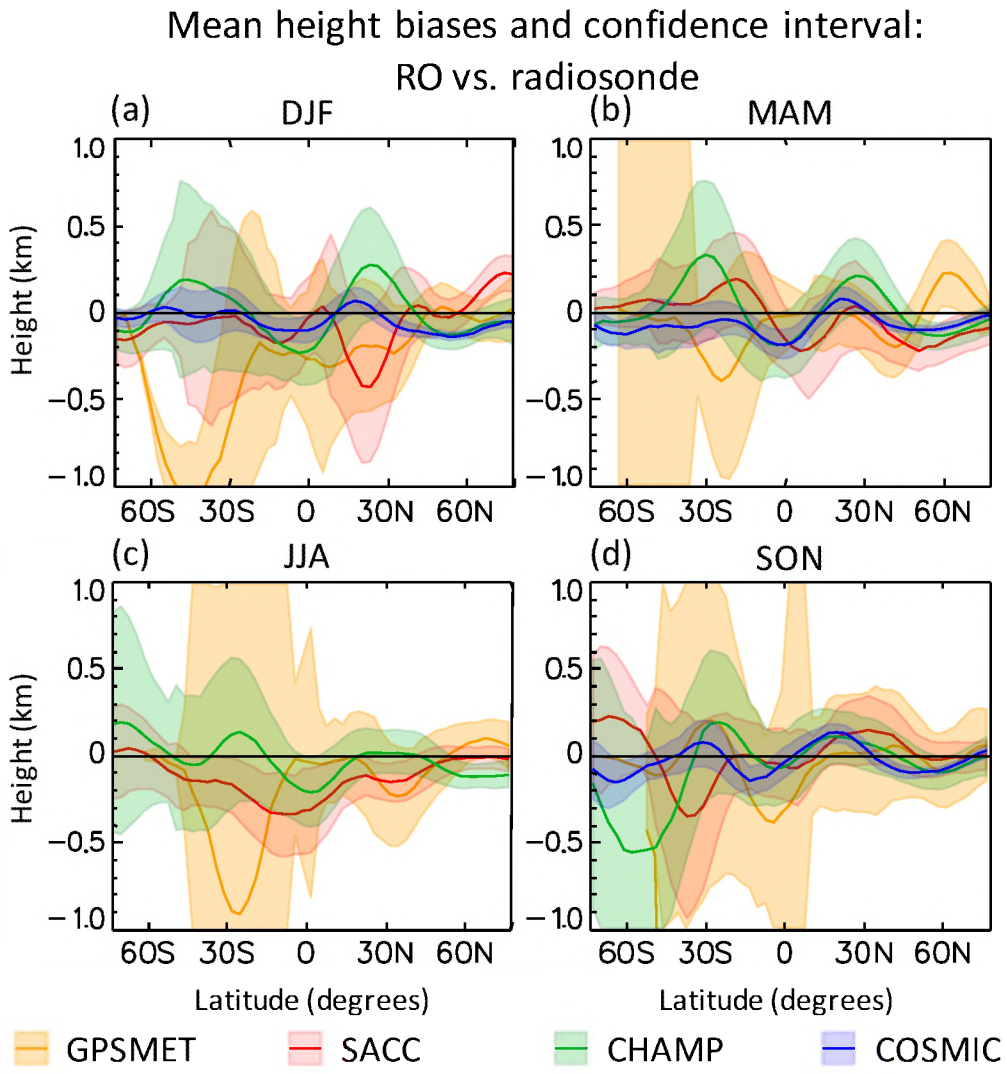

Figure 5. Zonal mean geopotential height differences between RO and radiosonde datasets, and the 95% confidence interval for the mean. Profiles are shown for DJF (a), MAM (b), JJA (c), and SON (d). All values are Gaussian smoothed over 30° latitude.

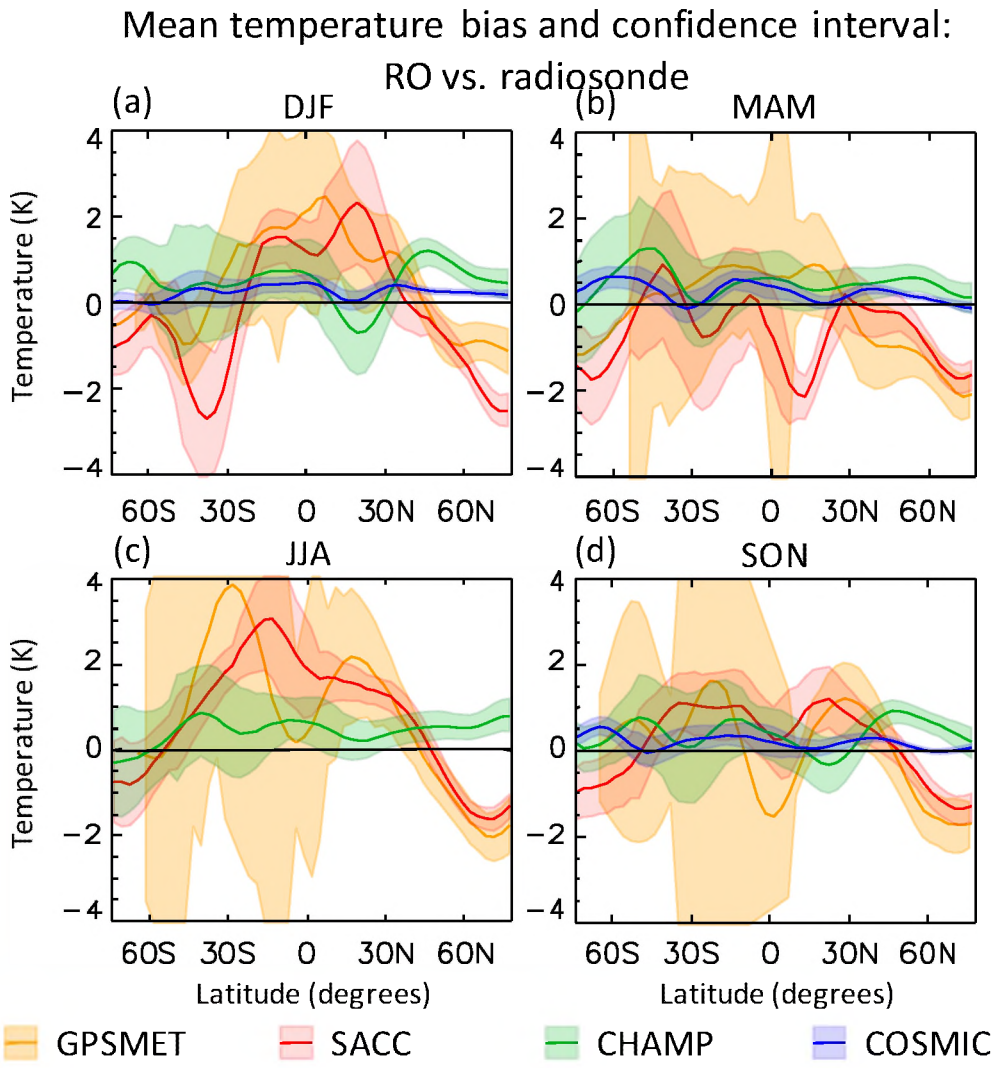

Figure 6. Zonal mean temperature differences between RO and radiosonde datasets, and the 95% confidence interval for the mean. Profiles are shown for DJF (a), MAM (b), JJA (c), and SON (d). All values are Gaussian smoothed over 30° latitude.

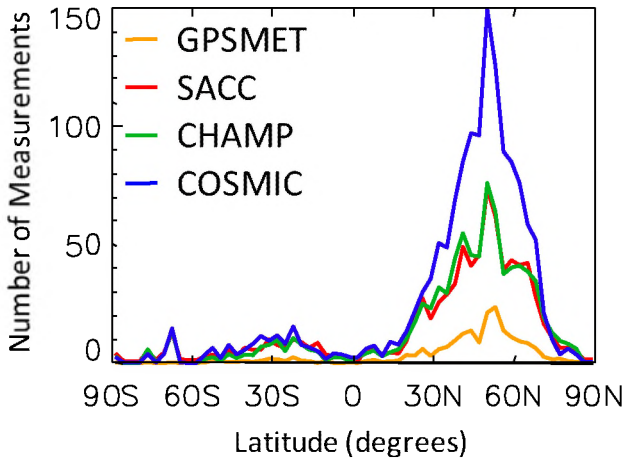

Figure 7. Meridional distribution of the average number of matching RO vs. radiosonde measurements per season for each RO instrument during the course of our study.

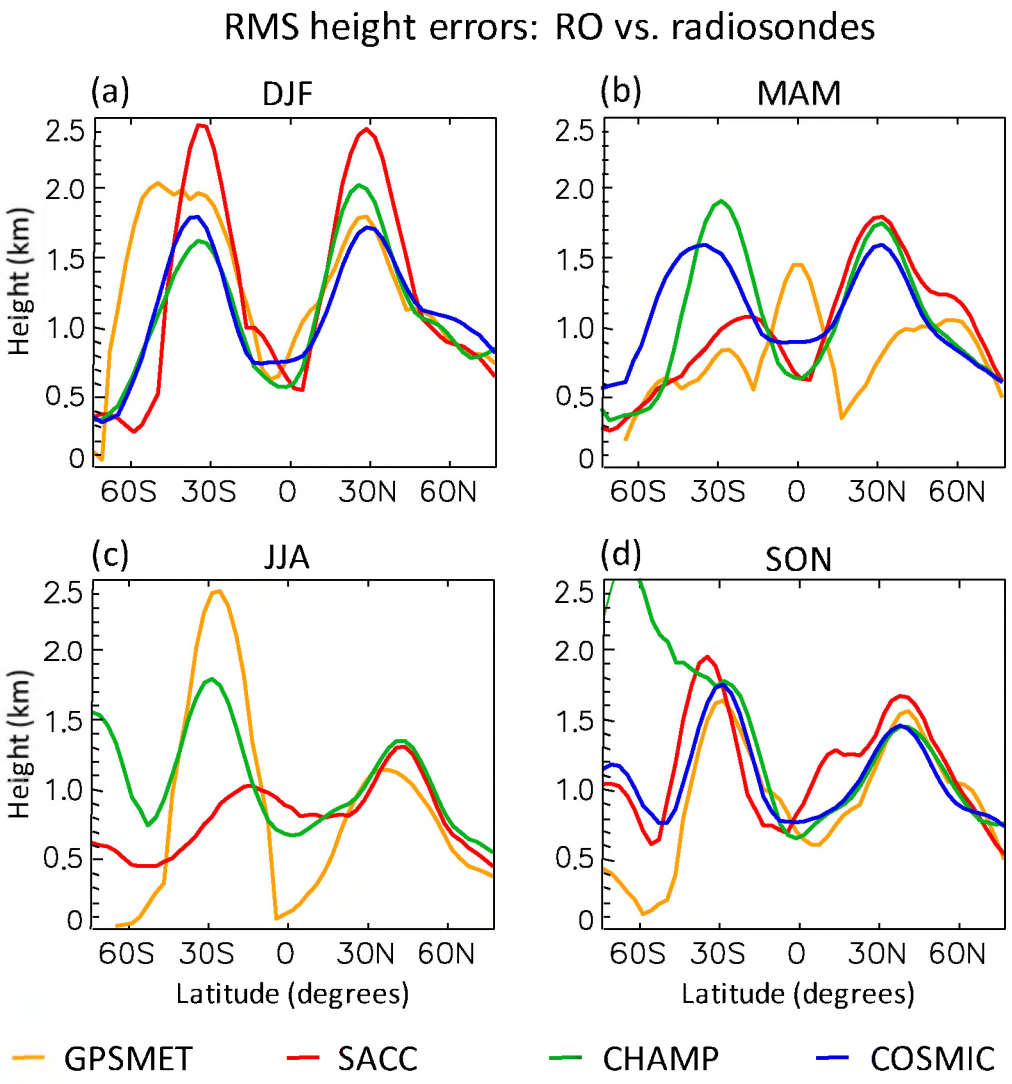

Figure 8. Meridional profile of RMS height differences between RO and radiosonde data. Profiles are shown for DJF (a), MAM (b), JJA (c), and SON (d). All values are Gaussian smoothed over 30° latitude.

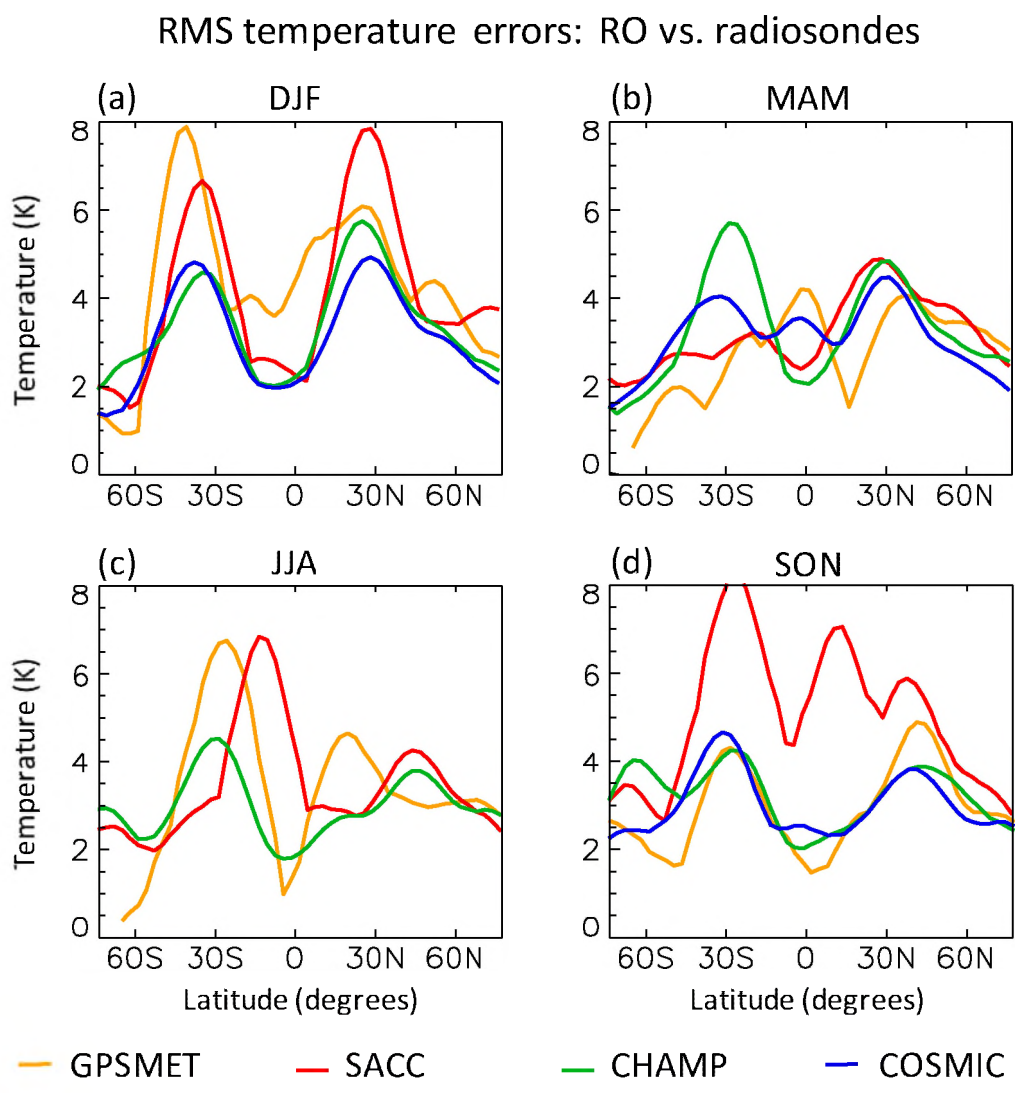

675 **Figure 9.** Meridional profile of RMS temperature differences between RO and radiosonde data. Profiles are shown for DJF (a), MAM (b), JJA (c), and SON (d). All values are Gaussian smoothed over 30° latitude.

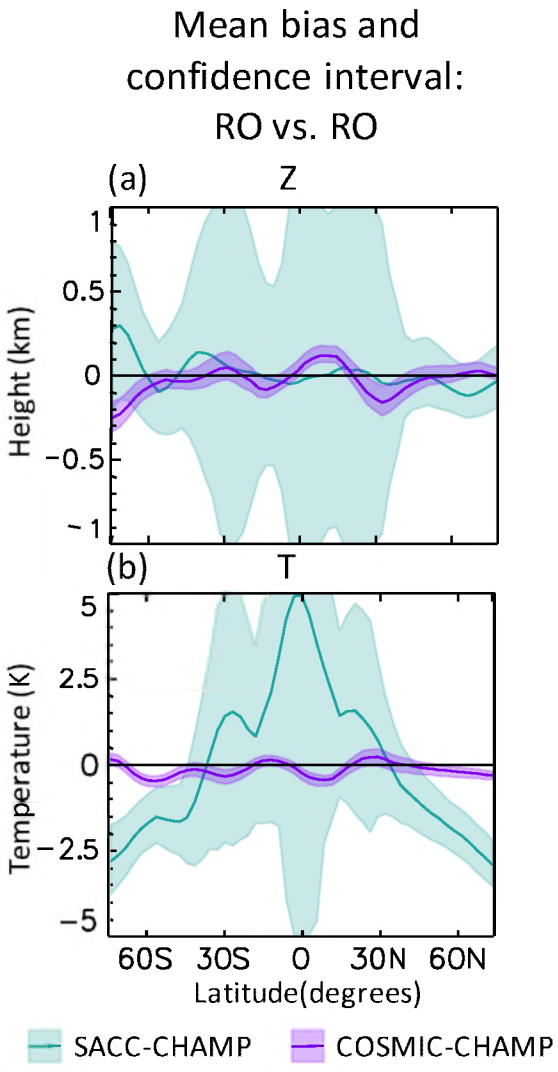

Figure 10. Zonal mean geopotential height differences (a) and temperature differences (b) between the RO datasets specified for SON. All values are Gaussian smoothed over 30° latitude.

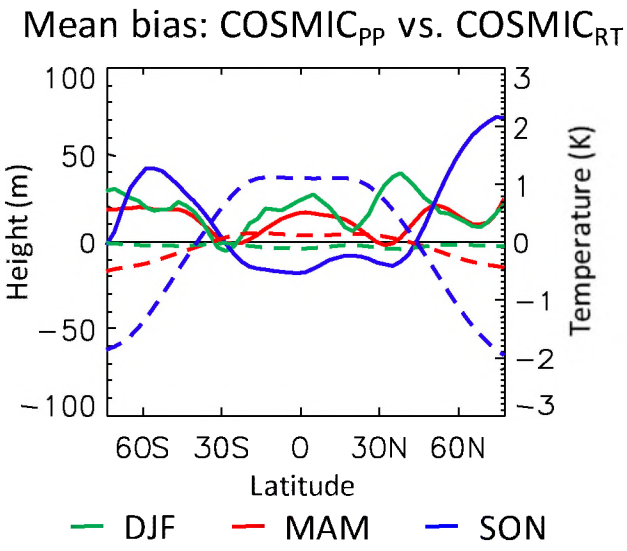

Figure 11. Zonal mean temperature differences between post-processed (PP) and near-real-time (RT) COSMIC data for the seasons shown. Solid lines and left axes show mean height differences, while dashed lines and right axes show mean temperature differences. All values are Gaussian smoothed over 30° latitude.

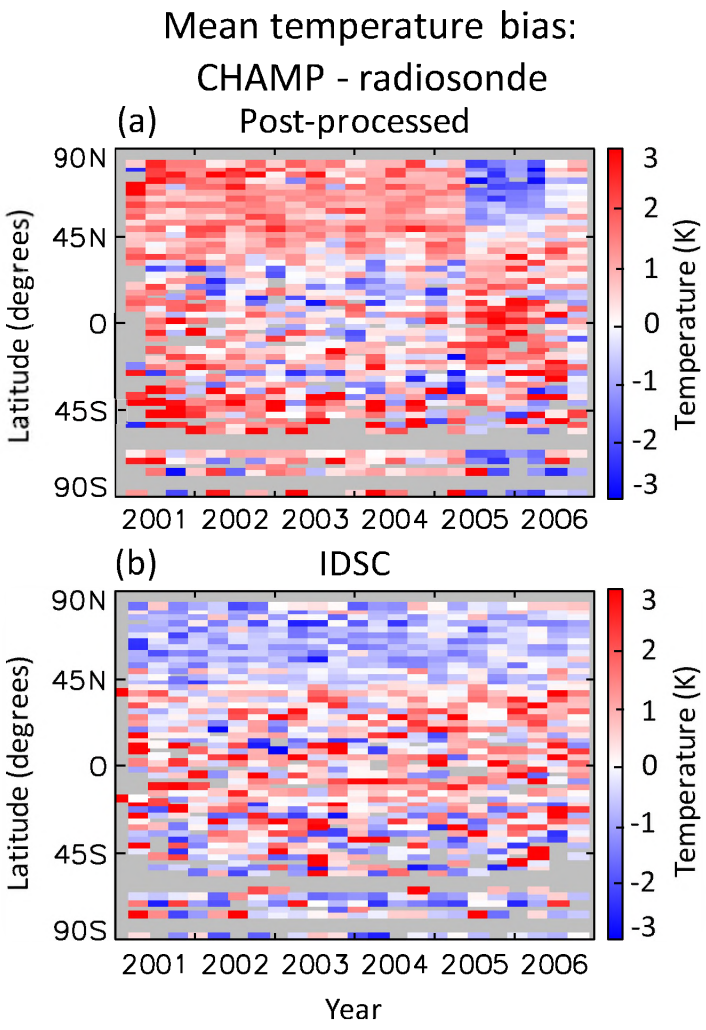

Figure 12. Zonal mean tropopause temperature bias between CHAMP and radiosonde data as a function of time and for two different processing methods. Shown are CHAMP biases from CDAAC (a) and ISDC (b).

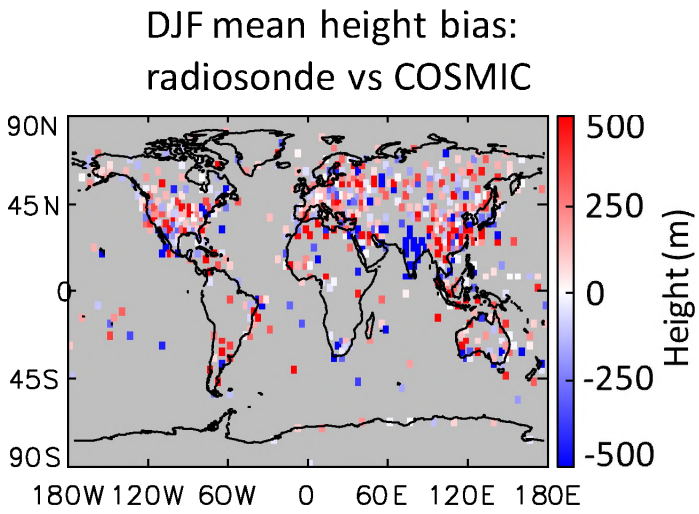

Figure13. Geographical distribution of mean tropopause height biases between radiosonde and COSMIC data during the period Dec. 2006 – Feb. 2007. Gray cells represent insufficient data.